Physics Letters B 669 (2008) 345–351

Contents lists available at ScienceDirect

Physics Letters B

www.elsevier.com/locate/physletb

Charge distributions in transverse coordinate space and in impact parameter space

Dae Sung Hwang [a,*], Dong Soo Kim [b], Jonghyun Kim [a]

[a] Department of Physics, Sejong University, Seoul 143–747, South Korea
[b] Department of Physics, Kangnung National University, Kangnung 210-702, South Korea

ARTICLE INFO

Article history:
Received 5 June 2008
Received in revised form 3 October 2008
Accepted 8 October 2008
Available online 14 October 2008
Editor: W. Haxton

PACS:
12.39.Ki
13.40.Gp
13.60.-r
14.20.Dh

ABSTRACT

We study the charge distributions of the valence quarks inside nucleon in the transverse coordinate space, which is conjugate to the transverse momentum space. We compare the results with the charge distributions in the impact parameter space.

1. Introduction

In recent years the role of the transverse momentum of the parton has been more important in the field of the hadron physics since it provides time-odd distribution and fragmentation functions, and makes the single-spin asymmetries (SSA) in hadronic processes possible [1–3]. One gluon exchange in the final state interactions (FSI) has been understood as a mechanism for generating a transverse single-spin asymmetry [3]. This FSI can be effectively taken into account by introducing an appropriate Wilson line phase factor in the definition of the distribution functions of quarks in the nucleon [4–7]. It is possible when the distribution functions are functions of the transverse momenta of the partons, as well as the longitudinal momentum fractions. Therefore, including the transverse momentum of the parton into consideration enlarges the realm of the investigation of the nucleon structure.

In Ref. [3] a simple scalar diquark model was used to demonstrate explicitly that the FSI can indeed give rise to a leading-twist transverse SSA, which emerged from interference between spin dependent amplitudes with different nucleon spin states. In Refs. [3,8] it was observed that the same overlap integrals between light-cone wavefunctions that describe the anomalous magnetic moment also appear in the expression of the Sivers distribution function with an additional factor in the integrand. Since these integrals are the overlaps between light-cone wavefunctions whose orbital angular momenta differ by $\Delta L^z = \pm 1$, the orbital angular momentum of the quark inside the proton is essential for the existence of the Sivers asymmetry.

In Refs. [9,10] the single-spin asymmetries were analyzed in the impact parameter space, in particular, the transverse distortion of parton distributions [11,12] was used to develop a physical explanation for the sign of the SSAs for transversely polarized targets. These aspects were illustrated explicitly by using the scalar diquark model in Ref. [13]. Besides these works, there have been a lot of important progresses of investigating the nucleon structure using the impact parameter space, for example, in Refs. [14–17]. Recently, Miller obtained the charge distributions in the impact parameter space for the valence quarks inside nucleon and found that the charge density inside neutron is negative at the center [18]. The term 'impact parameter space' in this Letter means that defined in these references.

In this Letter we study the transverse coordinate space of the parton which is the Fourier conjugate to the transverse momentum space. We investigate the charge distributions in the transverse coordinate space of the valence quarks inside proton and neutron, and compare them with those in the impact parameter space [18]. We present the results in terms of the scalar diquark model [3] for simplicity of presentation, however, extending to more general systems is straightforward. We also show the difference of the charge distributions in the transverse coordinate space and those in the impact parameter space clearly by using an explicit example of scalar diquark model.

* Corresponding author.
E-mail address: dshwang@slac.stanford.edu (D.S. Hwang).

0370-2693/$ – see front matter
doi:10.1016/j.physletb.2008.10.012

For explicit calculations we use the light-cone wavefunctions. The light-cone (LC) Fock representation of composite systems such as hadrons in QCD has a number of remarkable properties. Because the generators of certain Lorentz boosts are kinematical, knowing the wavefunction in one frame allows one to obtain it in any other frame [19,20]. One can construct any electromagnetic, electroweak, or gravitational form factor or local operator product matrix element of a composite or elementary system from the overlap of the LC wavefunctions [21–23]. LC wavefunctions also provide a convenient representation of the generalized parton distributions in terms of overlap integrals [24–26]. In this Letter we can study the charge distributions in the transverse coordinate space efficiently in the light-cone framework.

2. Charge distributions in transverse coordinate space

We consider a scalar diquark model which is an effective composite system composed of a fermion and a neutral scalar based on the one-loop quantum fluctuations of Yukawa theory. The light-cone wavefuctions describe off-shell particles but are computable explicitly from perturbation theory [23,26].

The $J^z = +\frac{1}{2}$ two-particle Fock state is given by

$$\left|\Psi^{\uparrow}_{\text{two particle}}(P^+, \mathbf{P}_\perp = \mathbf{0}_\perp)\right\rangle = \int \frac{\mathrm{d}^2\mathbf{k}_\perp\,\mathrm{d}x}{\sqrt{x(1-x)}16\pi^3}\left[\psi^{\uparrow}_{+\frac{1}{2}}(x,\mathbf{k}_\perp)\left|+\frac{1}{2}; xP^+, \mathbf{k}_\perp\right\rangle + \psi^{\uparrow}_{-\frac{1}{2}}(x,\mathbf{k}_\perp)\left|-\frac{1}{2}; xP^+, \mathbf{k}_\perp\right\rangle\right], \tag{1}$$

where

$$\begin{cases} \psi^{\uparrow}_{+\frac{1}{2}}(x,\mathbf{k}_\perp) = \frac{(xM+m)}{x}\varphi(x,\mathbf{k}_\perp), \\ \psi^{\uparrow}_{-\frac{1}{2}}(x,\mathbf{k}_\perp) = -\frac{(+k^1+ik^2)}{x}\varphi(x,\mathbf{k}_\perp), \end{cases} \tag{2}$$

in terms of a scalar function $\varphi(x,\mathbf{k}_\perp)$. This scalar function arises from the spectator propagator in a triangle Feynman diagram [22,23] and so the underlying Lorentz symmetry is respected. We generalize $\varphi(x,\mathbf{k}_\perp)$ by an adjustment of its power behavior p:

$$\varphi(x,\mathbf{k}_\perp) = \frac{gM^{2p}}{\sqrt{1-x}}x^{-p}\left(M^2 - \frac{\mathbf{k}_\perp^2+m^2}{x} - \frac{\mathbf{k}_\perp^2+\lambda^2}{1-x}\right)^{-p-1}, \tag{3}$$

where M, λ and m are the proton, spectator, and quark masses, respectively. The Yukawa theory result is for $p=0$, and Eq. (3) has an additional factor $M^{2p}x^{-p}(M^2 - \frac{\mathbf{k}_\perp^2+m^2}{x} - \frac{\mathbf{k}_\perp^2+\lambda^2}{1-x})^{-p}$ compared to the scalar function for the Yukawa model presented in Ref. [23]. In this additional factor, M^{2p} is attached for the dimensional purpose and the remaining factor can be induced from a Lorentz invariant form factor $(k^2-m^2)^{-p}$ at the quark–diquark vertex as in Ref. [27].

Similarly, the $J^z = -\frac{1}{2}$ two-particle Fock state is given by

$$\left|\Psi^{\downarrow}_{\text{two particle}}(P^+, \mathbf{P}_\perp = \mathbf{0}_\perp)\right\rangle = \int \frac{d^2\mathbf{k}_\perp\,\mathrm{d}x}{\sqrt{x(1-x)}16\pi^3}\left[\psi^{\downarrow}_{+\frac{1}{2}}(x,\mathbf{k}_\perp)\left|+\frac{1}{2}; xP^+, \mathbf{k}_\perp\right\rangle + \psi^{\downarrow}_{-\frac{1}{2}}(x,\mathbf{k}_\perp)\left|-\frac{1}{2}; xP^+, \mathbf{k}_\perp\right\rangle\right], \tag{4}$$

where

$$\begin{cases} \psi^{\downarrow}_{+\frac{1}{2}}(x,\mathbf{k}_\perp) = \frac{(+k^1-ik^2)}{x}\varphi(x,\mathbf{k}_\perp), \\ \psi^{\downarrow}_{-\frac{1}{2}}(x,\mathbf{k}_\perp) = \frac{(xM+m)}{x}\varphi(x,\mathbf{k}_\perp). \end{cases} \tag{5}$$

In (2) and (5) we have generalized the framework of the Yukawa theory by assigning a mass M to the external electrons, but a different mass m to the internal quark (fermion) line and a mass λ to the internal diquark (boson) line [21]. The idea behind this is to model the structure of a composite fermion state with mass M by a fermion and a boson constituent with respective masses m and λ.

The LC wavefunction in the transverse coordinate space $\tilde{\psi}(x,\mathbf{r}_\perp)$ is given by the Fourier transformation of $\psi(x,\mathbf{k}_\perp)$:

$$\psi(x,\mathbf{k}_\perp) = \int d^2\mathbf{r}_\perp \exp[-i\mathbf{k}_\perp\cdot\mathbf{r}_\perp]\tilde{\psi}(x,\mathbf{r}_\perp), \qquad \tilde{\psi}(x,\mathbf{r}_\perp) = \int \frac{d^2\mathbf{k}_\perp}{(2\pi)^2}\exp[i\mathbf{k}_\perp\cdot\mathbf{r}_\perp]\psi(x,\mathbf{k}_\perp). \tag{6}$$

From (6) we have the relation

$$\int \frac{d^2\mathbf{k}_\perp}{(2\pi)^2}\psi^*(x,\mathbf{k}_\perp)\psi(x,\mathbf{k}_\perp) = \int d^2\mathbf{r}_\perp\,\tilde{\psi}^*(x,\mathbf{r}_\perp)\tilde{\psi}(x,\mathbf{r}_\perp). \tag{7}$$

(2), (5) and (6) give the following light-cone wavefunctions in the transverse coordinate space:

$$\begin{cases} \tilde{\psi}^{\uparrow}_{+\frac{1}{2}}(x,\mathbf{r}_\perp) = (xM+m)\frac{r_\perp}{A_R}\frac{gM^2}{4\pi}(1-x)^{\frac{3}{2}}K_1(r_\perp A_R), \\ \tilde{\psi}^{\uparrow}_{-\frac{1}{2}}(x,\mathbf{r}_\perp) = -i(r^1+ir^2)\frac{gM^2}{4\pi}(1-x)^{\frac{3}{2}}K_0(r_\perp A_R), \end{cases} \tag{8}$$

and

$$\begin{cases} \tilde{\psi}^{\downarrow}_{+\frac{1}{2}}(x,\mathbf{r}_\perp) = i(r^1-ir^2)\frac{gM^2}{4\pi}(1-x)^{\frac{3}{2}}K_0(r_\perp A_R), \\ \tilde{\psi}^{\downarrow}_{-\frac{1}{2}}(x,\mathbf{r}_\perp) = (xM+m)\frac{r_\perp}{A_R}\frac{gM^2}{4\pi}(1-x)^{\frac{3}{2}}K_1(r_\perp A_R), \end{cases} \tag{9}$$

where $\mathbf{r}_\perp = (r^1, r^2)$, $r_\perp = |\mathbf{r}_\perp|$ and

$$A_R^2 = -M^2x(1-x) + m^2(1-x) + \lambda_R{}^2x, \quad R = u \text{ or } d. \tag{10}$$

Then, in the scalar diquark model the distribution in the transverse momentum space and that in the transverse coordinate space are given, respectively, by

$$P(\mathbf{k}_\perp) = \int dx\, P(x,\mathbf{k}_\perp) = \int \frac{dx}{(2\pi)^2}\big[\psi^{\uparrow\,*}_{+\frac{1}{2}}(x,\mathbf{k}_\perp)\psi^{\uparrow}_{+\frac{1}{2}}(x,\mathbf{k}_\perp) + \psi^{\uparrow\,*}_{-\frac{1}{2}}(x,\mathbf{k}_\perp)\psi^{\uparrow}_{-\frac{1}{2}}(x,\mathbf{k}_\perp)\big], \tag{11}$$

$$P(\mathbf{r}_\perp) = \int dx\, P(x,\mathbf{r}_\perp) = \int dx\big[\tilde\psi^{\uparrow\,*}_{+\frac{1}{2}}(x,\mathbf{r}_\perp)\tilde\psi^{\uparrow}_{+\frac{1}{2}}(x,\mathbf{r}_\perp) + \tilde\psi^{\uparrow\,*}_{-\frac{1}{2}}(x,\mathbf{r}_\perp)\tilde\psi^{\uparrow}_{-\frac{1}{2}}(x,\mathbf{r}_\perp)\big]. \tag{12}$$

3. Comparison of charge distributions in transverse coordinate and impact parameter spaces

Miller calculated the parton charge densities of nucleons by using the formula [18]

$$\rho^{\rm Imp}(\mathbf{b}_\perp) = \int \frac{d^2\mathbf{q}_\perp}{(2\pi)^2}\exp[i\mathbf{q}_\perp\cdot\mathbf{b}_\perp]F_1(\mathbf{q}_\perp). \tag{13}$$

In this section we interpret this $\rho^{\rm Imp}(\mathbf{b}_\perp)$ in terms of the LC wavefunctions and compare it with the charge density in the transverse coordinate space $P(\mathbf{r}_\perp)$ given in (12).

The fact that certain amplitudes that are convolutions in momentum space become diagonal in position space can be easily understood on the basis of some elementary theorems about convolutions and Fourier transforms. For example, if

$$f(\mathbf{k}_\perp) = \int d^2\mathbf{r}_\perp \exp[-i\mathbf{k}_\perp\cdot\mathbf{r}_\perp]\tilde f(\mathbf{r}_\perp), \qquad g(\mathbf{k}_\perp) = \int d^2\mathbf{r}_\perp \exp[-i\mathbf{k}_\perp\cdot\mathbf{r}_\perp]\tilde g(\mathbf{r}_\perp), \tag{14}$$

then the "form factor"

$$F(\mathbf{q}_\perp) \equiv \int \frac{d^2\mathbf{k}_\perp}{(2\pi)^2} f^*(\mathbf{k}_\perp-\mathbf{q}_\perp)g(\mathbf{k}_\perp) \tag{15}$$

becomes diagonal in Fourier conjugate space,

$$\int \frac{d^2\mathbf{q}_\perp}{(2\pi)^2}\exp[i\mathbf{q}_\perp\cdot\mathbf{r}_\perp]F(\mathbf{q}_\perp) = \tilde f^*(\mathbf{r}_\perp)\tilde g(\mathbf{r}_\perp). \tag{16}$$

This well-known result forms the basis for the interpretation of non-relativistic form factors as charge distributions in position space.

On the other hand, for

$$G(\mathbf{q}_\perp) \equiv \int \frac{d^2\mathbf{k}_\perp}{(2\pi)^2} f^*(\mathbf{k}_\perp - a\mathbf{q}_\perp)g(\mathbf{k}_\perp), \tag{17}$$

we have

$$\int \frac{d^2\mathbf{q}_\perp}{(2\pi)^2}\exp[i\mathbf{q}_\perp\cdot\mathbf{b}_\perp]G(\mathbf{q}_\perp) = \frac{1}{|a|^2}\tilde f^*\left(\frac{\mathbf{b}_\perp}{a}\right)\tilde g\left(\frac{\mathbf{b}_\perp}{a}\right). \tag{18}$$

$F_1(\mathbf{q}_\perp)$ can be expressed as

$$F_1(\mathbf{q}_\perp) = \int dx\, H(x,0,\mathbf{q}_\perp) = \int \frac{d^2\mathbf{k}_\perp\, dx}{(2\pi)^2}\big[\psi^{\uparrow\,*}_{+\frac{1}{2}}(x,\mathbf{k}'_\perp)\psi^{\uparrow}_{+\frac{1}{2}}(x,\mathbf{k}_\perp) + \psi^{\uparrow\,*}_{-\frac{1}{2}}(x,\mathbf{k}'_\perp)\psi^{\uparrow}_{-\frac{1}{2}}(x,\mathbf{k}_\perp)\big], \tag{19}$$

where $P' = P + q$ and

$$\mathbf{k}'_\perp = \mathbf{k}_\perp + (1-x)\mathbf{q}_\perp. \tag{20}$$

We note that in (19) we adopted the normalization of the wavefunction, with which $P(\mathbf{k}_\perp)$ in (11) satisfies $F_1(0) = \int d^2\mathbf{k}_\perp P(\mathbf{k}_\perp) = 1$.

Then, for $\rho^{\rm Imp}(\mathbf{b}_\perp)$ given in (13), we have

$$\begin{aligned}\rho^{\rm Imp}(\mathbf{b}_\perp) &= \int dx\,\rho^{\rm Imp}(x,\mathbf{b}_\perp)\\ &= \int \frac{d^2\mathbf{q}_\perp}{(2\pi)^2}\exp[i\mathbf{q}_\perp\cdot\mathbf{b}_\perp]F_1(\mathbf{q}_\perp) = \int \frac{d^2\mathbf{q}_\perp}{(2\pi)^2}\exp[i\mathbf{q}_\perp\cdot\mathbf{b}_\perp]\int dx\, H(x,0,\mathbf{q}_\perp)\\ &= \int dx \frac{1}{(1-x)^2}\left[\tilde\psi^{\uparrow\,*}_{+\frac{1}{2}}\left(x,\frac{\mathbf{b}_\perp}{-1+x}\right)\tilde\psi^{\uparrow}_{+\frac{1}{2}}\left(x,\frac{\mathbf{b}_\perp}{-1+x}\right) + \tilde\psi^{\uparrow\,*}_{-\frac{1}{2}}\left(x,\frac{\mathbf{b}_\perp}{-1+x}\right)\tilde\psi^{\uparrow}_{-\frac{1}{2}}\left(x,\frac{\mathbf{b}_\perp}{-1+x}\right)\right],\end{aligned} \tag{21}$$

where $\tilde\psi(x,\mathbf{r}_\perp)$ is the Fourier conjugate to $\psi(x,\mathbf{k}_\perp)$ as defined in (6). From (21) we have

$$\rho^{\rm Imp}(x,\mathbf{b}_\perp) = \int \frac{d^2\mathbf{q}_\perp}{(2\pi)^2}\exp[i\mathbf{q}_\perp\cdot\mathbf{b}_\perp]H(x,0,\mathbf{q}_\perp) = \frac{1}{(1-x)^2}P\left(x,\frac{\mathbf{b}_\perp}{-1+x}\right), \tag{22}$$

where $P(x,\mathbf{r}_\perp)$ in transverse coordinate space is given in (12) as

$$P(x,\mathbf{r}_\perp) = \big[\tilde\psi^{\uparrow\,*}_{+\frac{1}{2}}(x,\mathbf{r}_\perp)\tilde\psi^{\uparrow}_{+\frac{1}{2}}(x,\mathbf{r}_\perp) + \tilde\psi^{\uparrow\,*}_{-\frac{1}{2}}(x,\mathbf{r}_\perp)\tilde\psi^{\uparrow}_{-\frac{1}{2}}(x,\mathbf{r}_\perp)\big]. \tag{23}$$

Eq. (22) shows clearly the relation between the parton charge density in the impact parameter $(x,\mathbf{b}_\perp)$ space $\rho^{\rm Imp}(x,\mathbf{b}_\perp)$ and the distribution in the transverse coordinate $(x,\mathbf{r}_\perp)$ space $P(x,\mathbf{r}_\perp)$. This relation given in (22) was already obtained on general grounds in the literature [12,13,15]. In the above we verified this relation in the diquark model and study it quantitatively in the next section.

In this Letter $P(x,\mathbf{r}_\perp)$ and $\rho^{\rm Imp}(x,\mathbf{b}_\perp)$ denote parton density distributions for u and d quarks inside proton, and charge distributions for proton (p) and neutron (n). That is, $P_p=\frac{4}{3}P_u-\frac{1}{3}P_d$ and $P_n=\frac{2}{3}P_d-\frac{2}{3}P_u$ from the isospin symmetry, and the same relations for $\rho^{\rm Imp}(x,\mathbf{b}_\perp)$'s.

4. Explicit example with scalar diquark model

Using the scalar diquark model given in (2), (3) and (5), we fit the parameterization of Ref. [28] for the experimental results of the Dirac form factors $F_1(q^2)$ of nucleons. The parameterization of [29] is very similar to [28]. We use $p=1$ in (3). The fitting of the Dirac form factors of u and d quarks in proton with $m=0.5$ GeV, $\lambda_u=0.63$ GeV and $\lambda_d=0.535$ GeV are shown in Fig. 1, where the dotted lines are experimental results parameterized in [28] and the solid lines are those from (19) with these fitted values of m, λ_u and λ_d.

Fig. 2 presents the results of $P(\mathbf{r}_\perp)$ and $\rho^{\rm Imp}(\mathbf{b}_\perp)$ for u and d quarks inside proton, which are obtained by using the LC wavefunctions (2), (5), (8) and (9). The dash–dot lines are graphs of $P(\mathbf{r}_\perp)$ from (12) and the solid lines are $\rho^{\rm Imp}(\mathbf{b}_\perp)$ obtained from the formula (13) with $F_1(\mathbf{q}_\perp)$ given by using (19). In the figures ρ represents $\rho^{\rm Imp}$. Fig. 3 presents the charge distributions inside proton and neutron from the results of Fig. 2 by using $P_u=P_p+P_n/2$, $P_d=P_p+2P_n$ from the isospin symmetry, and the same relations for $\rho^{\rm Imp}(x,\mathbf{b}_\perp)$'s.

Figs. 2 and 3 show that $P(\mathbf{r}_\perp)$ extends toward outside further than $\rho^{\rm Imp}(\mathbf{b}_\perp)$, which can be understood from the fact that $\mathbf{b}_\perp/(-1+x)$ appears in the place of $\mathbf{r}_\perp$ in Eqs. (21) and (22). This property is also shown clearly in Table 1 which presents the results of the average values of $|\mathbf{r}_\perp|$ and $|\mathbf{b}_\perp|$.

We could see the difference between $P(\mathbf{r}_\perp)$ and $\rho^{\rm Imp}(\mathbf{b}_\perp)$ explicitly in Figs. 2 and 3, and in Table 1. Furthermore, it should be useful to analyze both x and $\mathbf{r}_\perp/\mathbf{b}_\perp$ dependences of this property by comparing $P(x,\mathbf{r}_\perp)$ in (12) and $\rho^{\rm Imp}(x,\mathbf{b}_\perp)$ in (21). Figs. 4–7 present $P(x,\mathbf{r}_\perp)$ and $\rho^{\rm Imp}(x,\mathbf{b}_\perp)$ of u and d quarks inside proton, and proton and neutron, respectively. We can see in these figures that $P(x,\mathbf{r}_\perp)$ decreases

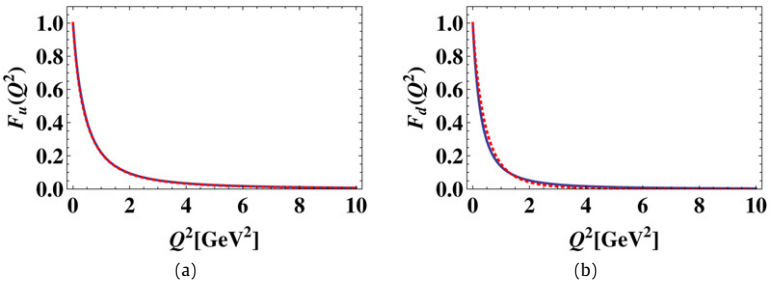

Fig. 1. The fitting of the Dirac form factors of u and d quarks in proton by using the scalar diquark model with $m=0.5$ GeV, $\lambda_u=0.63$ GeV and $\lambda_d=0.535$ GeV. The dotted lines are experimental results parameterized in [28] and the solid lines are those from (19) with the fitted parameter values.

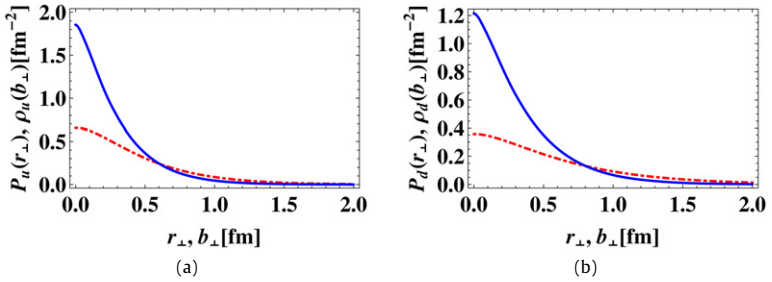

Fig. 2. The results of $P(\mathbf{r}_\perp)$ (dash–dot line) and $\rho^{\rm Imp}(\mathbf{b}_\perp)$ (solid line) for u and d quarks inside proton for the fitted scalar diquark model.

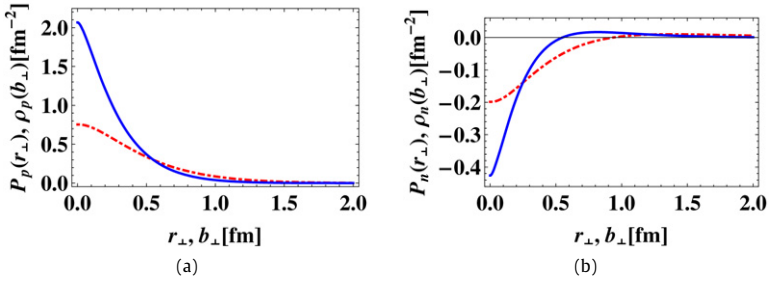

Fig. 3. The results of $P(\mathbf{r}_\perp)$ (dash–dot line) and $\rho^{\rm Imp}(\mathbf{b}_\perp)$ (solid line) for proton and neutron for the fitted scalar diquark model.

Table 1
The average values of $|\mathbf{r}_\perp|$ and $|\mathbf{b}_\perp|$ in fermi for the fitted scalar diquark model.

	u	d	p	n
$\langle\mathbf{r}_\perp\rangle$	0.77	1.08	0.67	0.21
$\langle\mathbf{b}_\perp\rangle$	0.50	0.61	0.46	0.07

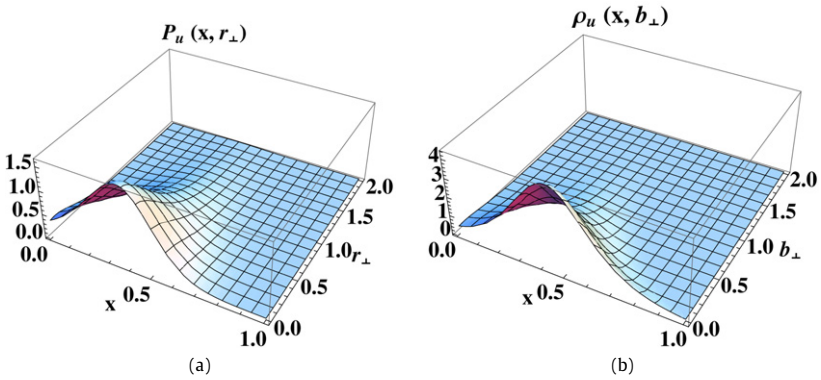

Fig. 4. $P(x, \mathbf{r}_\perp)$ and $\rho^{\rm Imp}(x, \mathbf{b}_\perp)$ of the u quark inside proton for the fitted scalar diquark model.

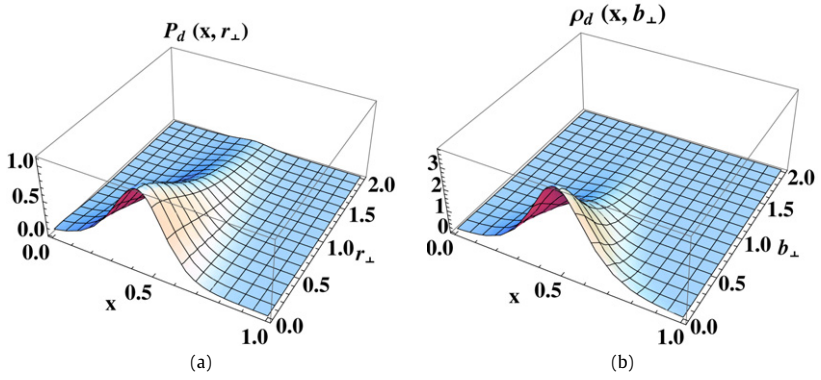

Fig. 5. $P(x, \mathbf{r}_\perp)$ and $\rho^{\rm Imp}(x, \mathbf{b}_\perp)$ of the d quark inside proton for the fitted scalar diquark model.

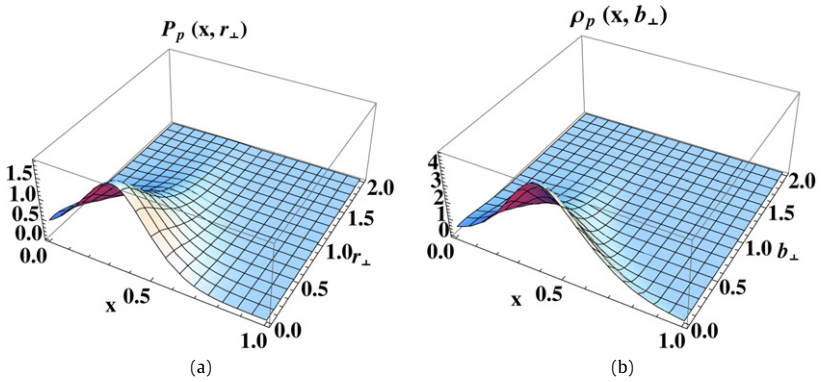

Fig. 6. $P(x, \mathbf{r}_\perp)$ and $\rho^{\rm Imp}(x, \mathbf{b}_\perp)$ of the proton for the fitted scalar diquark model.

more slowly than $\rho^{\rm Imp}(x, \mathbf{b}_\perp)$ when $\mathbf{r}_\perp$ and $\mathbf{b}_\perp$ increase. In order to show this property more clearly, we present in Fig. 8 their differences for a fixed value $x = 0.35$.

5. Conclusion

The transverse momentum dependent distribution functions provide detailed information on the nucleon structure. Then, it is natural to investigate at the same time the distribution functions also in the transverse coordinate space, in order to obtain the knowledge on the spatial structure of the nucleon. For this purpose there have been a lot of interesting studies on distribution functions in the impact parameter space, in particular in connection with the generalized parton distribution functions, and there have been many important progresses. However, it is desirable to understand better the relation of the impact parameter space to the transverse (spatial) coordinate space. In this Letter we showed explicitly in the scalar diquark model the relation between the charge distributions inside nucleon in the transverse coordinate space $P(x, \mathbf{r}_\perp)$ and those in the impact parameter space $\rho^{\rm Imp}(x, \mathbf{b}_\perp)$. The figures of the results show that $P(x, \mathbf{r}_\perp)$ decreases more slowly than $\rho^{\rm Imp}(x, \mathbf{b}_\perp)$ when $\mathbf{r}_\perp$ and $\mathbf{b}_\perp$ increase. This property can be understood from the fact that $\frac{\mathbf{b}_\perp}{(-1+x)}$ appears in the argument of $P(x, \mathbf{r}_\perp)$ in the formula given in (22): $\rho^{\rm Imp}(x, \mathbf{b}_\perp) = \frac{1}{(1-x)^2} P(x, \frac{\mathbf{b}_\perp}{-1+x})$. As a consequence, $P(\mathbf{r}_\perp)$ of (12) extends toward outside further than $\rho^{\rm Imp}(\mathbf{b}_\perp)$ of (13). The results in this Letter are also useful for the improvement of understanding the relation between the transverse coordinate space and the impact parameter space in general.

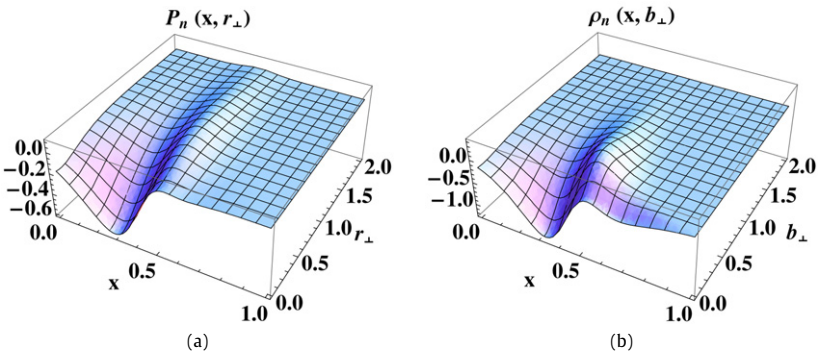

Fig. 7. $P(x, \mathbf{r}_\perp)$ and $\rho^{\rm Imp}(x, \mathbf{b}_\perp)$ of the neutron for the fitted scalar diquark model.

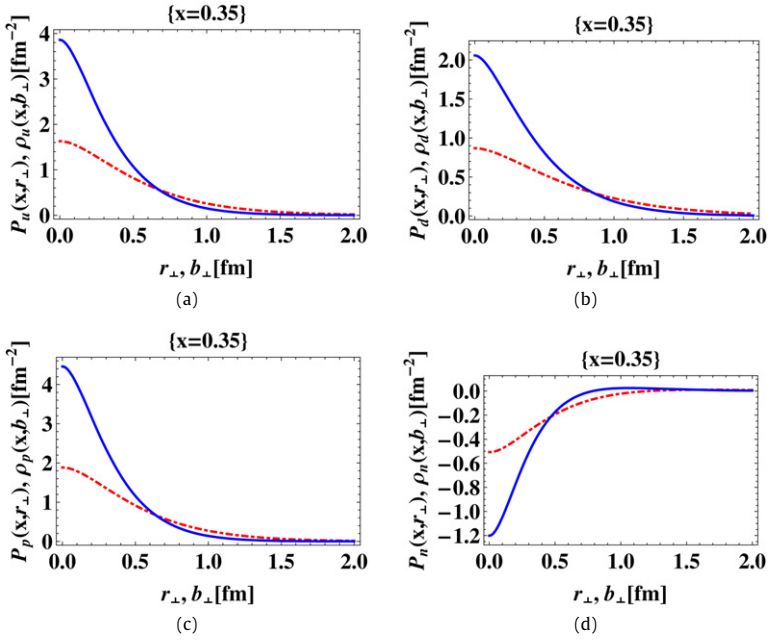

Fig. 8. $P(x = 0.35, \mathbf{r}_\perp)$ and $\rho^{\rm Imp}(x = 0.35, \mathbf{b}_\perp)$ of the u quark inside proton (a), the d quark inside proton (b), the proton (c), and the neutron (d) for the fitted scalar diquark model.

Acknowledgements

This work was supported in part by the International Cooperation Program of the KICOS (Korea Foundation for International Cooperation of Science & Technology), in part by the 2007 research fund from Kangnung National University, and in part by Seoul Fellowship.

References

[1] P.J. Mulders, R.D. Tangerman, Nucl. Phys. B 461 (1996) 197;
P.J. Mulders, R.D. Tangerman, Nucl. Phys. B 484 (1997) 538, Erratum.
[2] D. Boer, P.J. Mulders, Phys. Rev. D 57 (1998) 5780.
[3] S.J. Brodsky, D.S. Hwang, I. Schmidt, Phys. Lett. B 530 (2002) 99.
[4] D.W. Sivers, Phys. Rev. D 43 (1991) 261.
[5] J.C. Collins, Phys. Lett. B 536 (2002) 43.
[6] X. Ji, F. Yuan, Phys. Lett. B 543 (2002) 66.
[7] A.V. Belitsky, X. Ji, F. Yuan, Nucl. Phys. B 656 (2003) 165.
[8] S.J. Brodksy, D.S. Hwang, I. Schmidt, Phys. Lett. B 553 (2003) 223.
[9] M. Burkardt, Phys. Rev. D 66 (2002) 114005.
[10] M. Burkardt, Nucl. Phys. A 735 (2004) 185.
[11] M. Burkardt, Phys. Rev. D 62 (2000) 071503;
M. Burkardt, Phys. Rev. D 66 (2002) 119903, Erratum.
[12] M. Burkardt, Int. J. Mod. Phys. A 18 (2003) 173.
[13] M. Burkardt, D.S. Hwang, Phys. Rev. D 69 (2004) 074032.
[14] J.P. Ralston, B. Pire, Phys. Rev. D 66 (2002) 111501.
[15] M. Diehl, Eur. Phys. J. C 25 (2002) 223;
M. Diehl, Eur. Phys. J. C 31 (2003) 277, Erratum;
M. Diehl, Phys. Rep. 388 (2003) 41.
[16] A.V. Belitsky, D. Müller, Nucl. Phys. A 711 (2002) 118.
[17] S.J. Brodsky, D. Chakrabarti, A. Harindranath, A. Mukherjee, J.P. Vary, Phys. Lett. B 641 (2006) 440;

S.J. Brodsky, D. Chakrabarti, A. Harindranath, A. Mukherjee, J.P. Vary, Phys. Rev. D 75 (2007) 014003.
[18] G.A. Miller, Phys. Rev. Lett. 99 (2007) 112001.
[19] G.P. Lepage, S.J. Brodsky, Phys. Rev. D 22 (1980) 2157.
[20] S.J. Brodsky, H.-C. Pauli, S.S. Pinsky, Phys. Rep. 301 (1998) 299.
[21] S.J. Brodsky, S.D. Drell, Phys. Rev. D 22 (1980) 2236.
[22] S.J. Brodsky, D.S. Hwang, Nucl. Phys. B 543 (1999) 239.
[23] S.J. Brodsky, D.S. Hwang, B.Q. Ma, I. Schmidt, Nucl. Phys. B 593 (2001) 311.
[24] M. Diehl, T. Feldmann, R. Jakob, P. Kroll, Nucl. Phys. B 596 (2001) 33;
M. Diehl, T. Feldmann, R. Jakob, P. Kroll, Nucl. Phys. B 605 (2001) 647, Erratum.
[25] S.J. Brodksy, M. Diehl, D.S. Hwang, Nucl. Phys. B 596 (2001) 99.
[26] D.S. Hwang, D. Müller, Phys. Lett. B 660 (2008) 350.
[27] R. Jakob, P.J. Mulders, J. Rodrigues, Nucl. Phys. A 626 (1997) 937.
[28] J.J. Kelly, Phys. Rev. C 70 (2004) 068202.
[29] R. Bradford, A. Bodek, H. Budd, J. Arrington, Nucl. Phys. B (Proc. Suppl.) 159 (2006) 127.